JBC Papers in Press. Published on December 14, 2015 as Manuscript M115.664706
The latest version is at http://www.jbc.org/cgi/doi/10.1074/jbc.M115.664706

Suppressor of Cytokine Signaling-3 (SOCS-3) induces Proprotein Convertase Subtilisin Kexin Type 9 (PCSK9) expression in hepatic HepG2 cell line*

Massimiliano Ruscica[1], Chiara Ricci[1], Chiara Macchi[1], Paolo Magni[1,4], Riccardo Cristofani[1,5], Jingwen Liu[2], Alberto Corsini[1,3], and Nicola Ferri[6]

[1]Dipartimento di Scienze Farmacologiche e Biomolecolari, Università degli Studi di Milano, Milan, ITALY; [2]Department of Veterans Affairs Palo Alto Health Care System, Palo Alto, CA; [3]Multimedica IRCCS, Milan ITALY; [4]Centro per lo Studio delle Malattie Dismetaboliche e delle Iperlipemie - Enrica Grossi Paoletti, Università degli Studi di Milano, Milan, Italy; [5]Centro di Eccellenza per le Malattie Neurodegenerative, Università degli Studi di Milano, Milan, Italy; [6]Dipartimento di Scienze del Farmaco, Università degli Studi di Padova, Padua Italy

*Running title: *STAT3 dependent regulation of PCSK9*

To whom correspondence should be addressed: Nicola Ferri, Dipartimento di Scienze del Farmaco, Largo Meneghetti 2, 35131, Padua Italy, Phone: +39 0498275080, E-mail: nicola.ferri@unipd.it

Keywords: PCSK9, SOCS3, STAT, HepG2, insulin

Abstract: The suppressor of cytokine signaling (SOCS) proteins are negative regulators of the JAK/STAT pathway activated by pro-inflammatory cytokines, including the tumor necrosis factor-α (TNF-α). SOCS3 is also implicated in hypertriglyceridemia associated to insulin-resistance (IR). Proprotein Convertase Subtilisin Kexin Type 9 (PCSK9) levels are frequently found to be positively correlated to IR and plasma very low-density lipoprotein-triglycerides (VLDL-TG) concentrations. The present study aimed to investigate the possible role of TNF-α and JAK/STAT pathway on *de novo* lipogenesis and PCSK9 expression in HepG2 cells. TNF-α induced both SOCS3 and PCSK9 in a concentration-dependent manner. This effect was inhibited by transfection with siRNA anti-STAT3, suggesting the involvement of the JAK/STAT pathway. Retroviral overexpression of SOCS3 in HepG2 cells (HepG2^{SOCS3}) strongly inhibited STAT3 phosphorylation and induced PCSK9 mRNA and protein, with no effect on its promoter activity and mRNA stability. Consistently, siRNA anti-SOCS3 reduced PCSK9 mRNA levels while an opposite effect was observed with siRNA anti-STAT3. In addition, HepG2^{SOCS3} express higher mRNA levels of key enzymes involved in the *de novo* lipogenesis, such as fatty-acid synthase (FAS), stearoyl-CoA desaturase, and apo-B. These responses were associated with significant increase of SCD-1 protein, activation of SREBP-1, accumulation of cellular TG, and secretion of apoB. HepG2^{SOCS3} shows lower phosphorylation levels of IRS-1 Tyr^{896} and Akt Ser^{473} in response to insulin. Finally, insulin stimulation produced an additive effect with SOCS3 overexpression, further inducing PCSK9, SREBP-1, FAS and apoB mRNA. In conclusion, our data candidate PCSK9 as a gene involved in lipid metabolism regulated by pro-inflammatory cytokine TNF-α, in a SOCS3 dependent manner.

INTRODUCTION

The family of suppressor of cytokine signaling (SOCS) consists of eight members (SOCS-1 to SOCS-7 and CIS) all sharing a central SH2 domain and a C-terminal SOCS box. Expression of CIS, SOCS-1, SOCS-2 and SOCS-3 is induced by various cytokines, including IL-6 and TNF-α (1), and has been implicated in the negative regulation of several pathways, particularly the Janus kinase (JAK)-Signal Transducer and Activator of Transcription (STAT) one (2). SOCS proteins are highly and selectively induced in a tissue-specific manner by a diverse range of stimuli, other than the classical activators of the JAK/STAT pathway, including insulin (3), leptin (4), and resistin (5). In obesity, the expression of SOCS proteins is elevated in a variety of tissues that are vital for regulating fatty-acid (FA) metabolism and insulin sensitivity. For instance, SOCS1 and SOCS3 are upregulated in the liver of obese diabetic db/db mice and other insulin-resistance (IR) models, such as ob/ob mice and mice fed high-fat diet (6,7). The functional role of SOCS3 on hepatic steatosis and hyperlipidemia was also demonstrated by using SOCS antisense approach. The latter reduced in db/db mice the elevated hepatic lipid content and plasma triglycerides close to the normal observed in control mice (7). Furthermore, liver of morbidly obese subjects exhibits higher expression of SOCS3 protein and attenuated JAK/STAT signaling, resulting in enhanced sterol regulatory element binding protein-1c (SREBP-1c) transcriptional activity, a key regulator of *de novo* lipid biosynthesis (8). This evidence might suggest that the inhibition of JAK/STAT pathway by SOCS3 is mechanistically related to the development of hepatic IR and dyslipidemia in humans.

Proprotein Convestase Subtilisin Kexin Type 9 (PCSK9) belongs to the proprotein convertase family (9). Genetic and, more recently, pharmacological studies have clearly demonstrated its involvement in the regulation of low-density lipoprotein cholesterol (LDL) levels by inducing the degradation of the LDL receptor (LDLR) in a manner independent from its proteolytic activity (10-13). Similarly to the genes involved in the regulation of the cholesterol homeostasis, i.e. hydroxyl-methyl-glutaryl CoA reductase and synthase and the LDLR, PCSK9 is under the control of the SREBP-2 (14). For this reason, the pharmacological activation of the SREBP pathway by HMG-CoA reductase inhibitors, statins, induces PCSK9 both in experimental and clinical settings (15-17). While SREBP-1a and SREBP-1c preferentially activate genes involved in the synthesis of fatty acids and triglycerides, their homologous SREBP-2 preferentially transcribes for genes involved in the cholesterol biosynthetic pathway (18,19). To this regard, PCSK9 appears to be regulated by both SREBP-2 and SREBP-1c (14,20), where the latter mediating the induction of PCSK9 in response to insulin (14,21-23). The involvement of SREBP-1c in the regulation of PCSK9 levels has also been observed in humans, where PCSK9 levels positively correlated with IR, liver steatosis and very low density lipoprotein-triglycerides (VLDL-TG) (24).

This evidence suggests that, although PCSK9 is an important regulator of LDL-C levels, it could be also implicated in the homeostasis of TG-rich lipoproteins. It is, indeed, of interest that the association between plasma PCSK9 and LDL-C is weak and has been estimated to account for only the 7% of the variations in LDL-C (25), while PCSK9 levels are more significantly associated with plasma concentrations of TG, glucose and insulin (21,25-27). Based on these premises, the present study aimed to investigate the possible role of TNF-α and JAK/STAT pathway on *de novo* lipogenesis and PCSK9 expression in human HepG2 cell line.

EXPERIMENTAL PROCEDURES

Cell cultures - The Human hepatocellular liver carcinoma cell line, HepG2, was cultured in 10%FCS/MEM supplemented with penicillin (10,000 U/ml), streptomycin (10 mg/ml), nonessential amino acids and sodium pyruvate. For the experiments, cells were incubated with MEM containing either 10% of lipoprotein plasma deprived serum (LPDS) or 10% Fetal Calf Serum (FCS), as indicated in the figures legend.

Reagents and antibodies - MEM, trypsin EDTA, penicillin, streptomycin, nonessential amino acid

solution, FCS, disposable culture flasks and petri dishes were from Euroclone (Pero, Milan, Italy), and filters were from Millipore (Billerica, MA). Molecular weight protein standards were from BIO-RAD Laboratories (Hercules, CA). SDS, TEMED, ammonium persulfate, glycine, and acrylamide solution (30%T, 2.6%C) were obtained from BIO-RAD Laboratories. BCA assay for determination of protein concentrations was purchased from Thermo Fischer Scientific (Waltham, MA). [^{14}C]-Acetate were from Amersham (Cologno Monzese, Milan, Italy). Recombinant insulin, Tumor Necrosis Factor-α (TNF-α) and bovine serum albumin (BSA) were purchased from SIGMA-Aldrich (Milan, Italy). STAT3 inhibitor, MD77, was kindly provided by Prof. Daniela Barlocco (Università degli Studi di Milano, Milan, Italy) [31]. The JAK inhibitor JAK1 was purchased from Millipore (Millipore, Milan, Italy). Actinomycin D was purchased from Abcam (Cambridge, UK) and fatostatin hydrobromide and 25-hydroxycholesterol (25-OH cholesterol) from SIGMA-Aldrich (Milan ITALY). For Western Blot (WB) analysis, the following antibodies were used: anti-PCSK9 and anti SREBP-2 (Cayman, Tallinn, Estonia), anti-α-tubulin (SIGMA-Aldrich), anti-pAKT (Millipore); anti-AKT and anti-SOCS3 (Cell Signalling Tecnology, Danver, MA); anti-pSTAT3, anti-insulin receptor substrate (pIRS-1) and anti- stearoyl-CoA desaturase (SCD-1) and anti-hepatocyte nuclear factor (HNF)-1α (Abcam, Cambridge, UK); anti-STAT3 and SREBP-1 (Santa-Cruz Biotechnology, Santa Cruz, CA); anti-mouse and anti-rabbit peroxidase-conjugated secondary antibodies (Jackson ImmunoResearch Lab; Cambridgeshire, UK).

Animals - Four-week-old male ob/ob mice and their lean, wild-type male C57BL/6J controls were purchased from Charles River (Calco, Italy). In compliance with the Principles of Laboratory Animal Care (NIH publication 86-23), mice were housed at constant room temperature (23°C) in a 12-hour light/dark cycle (7 a.m. to 7 p.m) receiving standard chow and water *ad libitum*. Mice were sacrificed at fourteen weeks of age in the fasted state.

Generation of human SOCS3 expression construct and retroviral infection in HepG2 cells - Full-length human SOCS3 (accession no. 003955) was generated by polymerase chain reaction (PCR) using the following primers: 5'-CGGGATCCATGGTCACCCACAGCAAGTT TCC-3' and 5'-CGCTCGAGTTAAAGCGGG GCATCGTACTGG-3'and the Expand High-Fidelity PCR System (Roche Diagnostics, S.p.A, Monza, Italy). The sequence of the polymerase chain reaction generated construct was confirmed by sequencing (Primm, Milan, Italy). Retroviral expression plasmid was then constructed using the pBM-IRES-PURO (28) expressing the puromycin resistance gene as a selectable second cistron gene, generated from the original pBM-IRES-EGFP, generously provided by Garry P. Nolan (Stanford University, Stanford, CA). Retroviral infections of HepG2 were performed as previously described (28,29). A polyclonal population of HepG2 control and SOCS3 overexpressing cells have been than selected with 10 μg/ml of puromycin.

Transfection of siRNA - ON-TARGET plus SMART pool siRNA directed to STAT3 and SOCS3 or scramble control were purchased from Dharmacon™ (Carlo Erba Reagents, Milan, Italy). Transfections were performed as previously described using SilentFect™ Lipid Reagent (BIO-RAD laboratories, Hercules, CA) according to the manufacturer's protocol (30,31). HepG2 cells were seeded at a density of 6×10^5/well (6 well tray) the day before the transfection in completed medium. Cells were then transfected with 20 nM of siRNA for 48h then the medium replaced with MEM containing 5%LPDS ± TNF-α for an additional 24h before performing the quantitative (q)PCR or WB analysis.

Synthesis of total cholesterol - Cholesterol biosynthesis was estimated by measuring the incorporation of [^{14}C]-Acetate into cellular cholesterol, as previously described (32).

Evaluation of intracellular TG and Cholesterol levels - Total cellular lipids were extracted with hexane/isopropanol 3:2 and TG and Cholesterol contents were determined with enzymatic assays (HORIBA ABX, Montpellier, France).

ELISA assay. Conditioned media was cleared by centrifugation (13,000 rpm for 10 min.) and store at -20°C. The amount of apolipoprotein (apo) B (Vinci-Biochem, Firenze, Italy) and PCSK9 (R&D System, Minneapolis, MN) was then

quantified by using the ELISA assays according to manufacturer's instructions. The values were normalized with total cell protein contents, extracted from the cell monolayer, determined by BCA assay (Thermo Fischer Scientific).

Luciferase reported promoter activities assay - The plasmid pGL3-PCSK9-D4 contains the 5′ flanking region of the PCSK9 gene from -440 to -94, relative to the ATG start codon as previously described (33). To measure the PCSK9 promoter activity, HepG2 cells were seeded in 48 well plates at a density of 8×10^5 cells per well. On the next day, cells were transiently transfected with pGL3-PCSK9-D4 plasmids with turbofect reagent (Carlo Erba Reagents) and, 48h post transfection, cells were incubated with serum-free medium in the presence or absence of insulin (10^{-7}M) for an additional 24h. Luciferase activities were measured by using Neolite reagent (Perkin Elmer, Milan, Italy) according to manufacturer's instructions. pCMV-β vector, encoding for β-galactosidase, (Clontech Lab., mountain View, CA) was cotransfected as internal control. β-galactosidase activity was assayed as described (34). Luciferase activity was normalized to the β-galactosidase activity of the cotransfected pCMV-β construct.

RNA preparation and quantitative real time PCR- Total RNA was extracted with the iScript Sample Preparation Buffer (BIO-RAD laboratories) cDNA synthesis preparation reagents (BIO-RAD laboratories) according to manufacturer's instructions. Reverse transcription-polymerase first-strand cDNA synthesis was performed by using the iScript cDNA synthesis Kit (BIO-RAD laboratories). Quantitative real time PCR (qPCR) was then performed by using the Kit Thermo SYBR Green/ROX qPCR Master Mix (Carlo Erba Reagents) and specific primers for selected genes. Primer sequences used for qPCR analysis are shown in Table 1. The analyses were performed with the ABI Prism® 7000 Sequence Detection System (Applied Biosystems; Life Technologies Europe BV, Milan, Italy). PCR cycling conditions were as follows: 94°C for 3min, 40 cycles at 94°C for 15s, and 60°C for 1min. Data were expressed as Ct values and used for the relative quantification of targets with the ΔΔCt calculation.

Western Blot Analysis - Total cytosolic protein extracts of HepG2 and HepG2^{SOCS3}, were obtained by collecting cells in 150 µl of Mammalian Protein Extraction Reagents (Thermo Fisher Scientific) containing a cocktail of protease and phosphatase inhibitors (Roche Diagnostics). Twenty µg of proteins and a molecular mass marker (Novex® Sharp Protein Standard, InvitrogenTM; Life Technologies Europe BV) were separated on 4-12% sodium dodecylsulfate-polyacrylamide gel (SDS-PAGE; Novex® NuPAGE® 4-12% Bis-Tris Mini Gels, InvitrogenTM; Life Technologies) under denaturing and reducing conditions. Proteins were then transferred to a nitrocellulose membrane by using the iBlotTM Gel Transfer Device (InvitrogenTM; Life Technologies). The membranes were washed with Tris-Buffered Saline-Tween 20 (TBS-T) and non-specific binding sites were blocked in TBS-T containing 5% (BSA; Sigma-Aldrich) for 90 min at RT. The blots were incubated overnight at 4°C with a diluted solution (5% BSA or non-fat dried milk) of the following human primary antibodies: anti-PCSK9 (1:100); anti SREBP-2 (1:200) anti-pAKT, (1:100); anti-AKT (1:1,000); anti-pSTAT3 (1:10,000); anti-pIRS-1 (1:5,000); anti-SCD-1 (1:500); anti-STAT3 (1:1,000); anti-SREBP-1a (1:500); anti-SOCS3 (1:100); anti-HMG-CoA reductase (1:500); anti HNF-1α (1:1,000)and anti-α-tubulin (1:2,000). Membranes were washed with TBS-T and then exposed for 90 min at RT to a diluted solution (5% non-fat dried milk) of the secondary antibodies. Immunoreactive bands were detected by exposing the membranes to ClarityTM Western ECL chemiluminescent substrates (Bio-Rad Laboratories) for 5 min and images were acquired with a ChemiDocTM XRS System (Bio-Rad Laboratories). Densitometric readings were evaluated using the ImageLabTM software as previously described. The values of the phosphorylated proteins were normalized to those of the corresponding constitutive forms to express arbitrary units of relative expression.

Analysis of the data – Statistical analysis was performed using the Prism statistical analysis package version 6.0 (GraphPad Software, San Diego, CA). Data are given as mean ± SD of three independent experiments. When possible, p-values were determined by Student's t-test.

Otherwise, differences between treatment groups were evaluated by 1-way ANOVA. A probability value of $p<0.05$ was considered statistically significant.

RESULTS

TNF-α induces SOCS3 and PCSK9 in HepG2 cells - Release of pro-inflammatory cytokines, such as TNF-α and IL-6, from adipocytes of obese subjects with IR, has been shown to activate the JAK/STAT pathway at the hepatic levels and inducing, either directly or indirectly, the transcription of different target genes including SOCS proteins (6,7). In agreement with these observations, we found that the incubation of hepatic cell line HepG2 with TNF-α induced the expression of SOCS3 mRNA in a time- and concentration-dependent manner (Figure 1A), reaching the maximal induction after 24h incubation at the concentration of 10 ng/ml. This latter resulted in three-fold induction of SOCS3 protein, evaluated by WB analysis (Figure 1A). Under the same experimental conditions, TNF-α induced both PCSK9 mRNA, although to lower extent (Figure 1B), and PCSK9 protein (+41%), as determined by WB analysis (Figure 1B). Transfection of HepG2 cells with specific siRNA significantly down-regulated protein expression of STAT3 and SOCS3 (Figure 1C). siRNA STAT3 completely blocked the induction of SOCS3 by TNF-α (Figure 1D). A similar effect was observed on the expression levels of PCSK9, where siRNA to either SOCS3 or STAT3 blocked the effect of TNF-α (Figure 1E). These results suggest the possibility that TNF-α induces PCSK9 by inducing the SOCS3 expression.

SOCS3 overexpression induces PCSK9 in HepG2 - To further investigate the role of SOCS3 on PCSK9 expression, we generated a retrovirally transduced HepG2 cell line with a plasmid encoding human SOCS3 ($HepG2^{SOCS3}$). After puromycin selection, the mRNA and protein overexpression of exogenous human SOCS3, were evaluated by qPCR and WB analyses, respectively. $HepG2^{SOCS3}$ cells were compared with HepG2 transduced with empty retroviral vector encoding only the puromycin resistance gene. As shown in Figure 2A, retroviral transduction determined approximately 90-fold induction of mRNA of SOCS3 that translated into a 70% increase of protein SOCS3 (Figure 2B). The overexpression of SOCS3 abrogated basal STAT3 phosphorylation state (Figure 2C).

$HepG2^{SOCS3}$ cells show higher levels of PCSK9 mRNA (3.48±0.35 fold, Figure 2D) and increased amount of cellular and secreted PCSK9 (1.53 fold and 2.18±0.38 fold respectively; Figure 2E and 2F). Since SOCS3 has been shown to be up-regulated in animal models of obesity (6), we then evaluated the mRNA levels of PCSK9 and SOCS3 in the liver of ob/ob and wild-type C57BL/6 control mice. The ob/ob mice expressed higher levels of SOCS3 (6.46±4.8 fold) and this condition was associated with a significant induction of PCSK9 (2.03±1.54 fold) (Figure 2G and 2H).

The inhibition of SOCS3 and STAT3 by siRNA resulted in an opposite effect on PCSK9 mRNA levels, with a significant reduction after transfection with siRNA SOCS3 and an induction with siRNA STAT3 (Figure 2I).

We then investigated the effect of SOCS3 on PCSK9 promoter activity in HepG2 and $HepG2^{SOCS3}$ transfected with the luciferase reporter construct pGL3-PCSK9-D4 (33). This plasmid contains the 5′ flanking region of the PCSK9 gene, from nt -440 to -94 (relative to the ATG start codon), in front of the luciferase coding sequence. The relative luciferase activity of the PCSK9 promoter was not affected by the expression of SOCS3 in HepG2 cells (Figure 2L). A similar response was observed by using the D4 construct containing the mutation of sterol regulatory element (SRE), while the mutation of HNF-1 site determined a significant increase of the promoter activity in $HepG2^{SOCS3}$ cells, although the overall transcriptional activity was almost abolished (Figure 2L).

To further investigate the effect of SOCS3 on the PCSK9 mRNA induction, we determined the involvement of the SREBP factors by incubating HepG2 with 25-OH cholesterol (inhibitor of both SREBP-1 and SREBP-2) (32) or fatostatin (a more selective inhibitor of SREBP-1) (35). As shown in Figure 3A, 25-OH cholesterol, completely downregulated the PCSK9 mRNA levels in both HepG2 and $HepG2^{SOCS3}$. On the contrary, fatostatin affected exclusively the induction of PCSK9 in $HepG2^{SOCS3}$ (Figure 3B).

SOCS3 overexpression induced the processing from the precursor to the active form of SREBP-1 (Figure 3C). The activation of SREBP-2 was inhibited, with the accumulation of its precursor and a reduction of the active form (Figure 3C). In addition, HNF-1α protein (+54%) and mRNA levels (2.87±0.98 fold) were significantly induced in SOCS3 overexpressing cells (Figure 3C and 3D). The incubation with the transcriptional activity inhibitor, actinomycin D, showed that in HepG2^{SOCS3} the stability of PCSK9 mRNA was not affected compared to HepG2 (Figure 3E). Taken together, these results suggest that the PCSK9 induction in response to SOCS3 overexpression is mainly mediated by a transcriptional-regulated process.

Pharmacological inhibition of JAK/STAT pathway induces PCSK9. To further investigate the effect of STAT3 inhibition on PCSK9 expression, HepG2 cells were incubated with non-toxic concentration of STAT3-inhibitor MD77 (Figure 4) (36). Incubation of HepG2 cells for 48h with 10^{-7}M MD77, determined a very similar cellular responses than those observed with SOCS3 overexpression. In particular, incubation with MD77 induced fatty-acid synthase (FAS; 2.93±1.28 fold, Figure 4A), PCSK9 (2.06±0.7 fold, Figure 4B), and only marginally HMG-CoA reductase (1.58±0.2fold, Figure 4C), with a not statistically significant reduction of LDLR (-45.3±24.7%, Figure 4D). The JAK inhibitor, JAK1, significantly increased FAS (1.56±0.05 fold, Figure 4E), PCSK9 (3.30±0.32 fold, Figure 4F) and HMG-CoA reductase (1.49±0.09 fold, Figure 4G), and marginally reduced the LDLR (-43.2±24.2%, Figure 4H). Consistently with the results with HepG2^{SOCS3}, no effect on PCSK9 promoter activity was observed after 24h incubation with JAK1 (Figure 4I). Taken together, these results demonstrate that the inhibition of the JAK/STAT pathway induces PCSK9 in HepG2 cells.

SOCS3 overexpression induces de novo lipogenesis in HepG2 cells - Several *in vivo* evidence demonstrated the pivotal role of SOCS3 and STAT3 on lipid metabolism and SREBP-1 transcriptional activity (6,7,37). To verify that a similar response also occurs in our experimental model, we determined the mRNA levels of SREBP-1 target genes, such as FAS and SCD-1 and the levels of apoB. HepG2^{SOCS3} cells show higher mRNA levels of FAS (3.59±0.40 fold, Figure 5A) as well as that of SCD-1 gene (1.92±0.12 fold, Figure 5B) and protein (3.81±0.75 fold; Figure 5C). Together with these changes, we observed a significant increment of apoB mRNA (4.08±0.41 fold, Figure 5D), and protein in the conditioned media (3.47±0.09 fold, Figure 5E). Accumulation of intracellular TG levels (22.1±7.1μg/mg protein vs. 38.3±9.1μg/mg protein; Figure 5F) was seen in HepG2^{SOCS3}, with no significant changes in total cholesterol content (Figure 5G).

In response to TNF-α, we observed a significant induction of SCD-1, apoB and FAS mRNA levels (2.11±0.43, 1.60±0.33 and 1.39±0.21 fold, respectively; Figure 5H-L). These responses were reversed in HepG2 cells transfected with siRNA STAT3 (Figure 5H-L). Taken together, the overexpression of SOCS3 induces the *de novo* lipogenesis and increased apoB production in HepG2 cells, effects dependent by STAT3.

SOCS3 overexpression does not affect the cholesterol biosynthesis in HepG2 - A series of experiments were performed to determine the effect of SOCS3 on genes under the control of SREBP-2, such as HMG-CoA reductase and LDLR. HMG-CoA reductase mRNA was induced in HepG2^{SOCS3} cells (2.10±0.66 fold, Figure 6A); conversely, the LDLR mRNA levels were reduced in response to SOCS3 overexpression (-56%±21.6%, Figure 6B). These changes were not associated with significant variation of HMG-CoA reductase protein level (Figure 6C). The lack of significant changes of HMG-CoA reductase was also confirmed by the fact that the cholesterol biosynthesis was not altered in HepG2^{SOCS3} cells compared to HepG2 cells (Figure 6D).

Effect of SOCS3 overexpression on insulin-induced PCSK9 expression - To corroborate the pathophysiological relevance of our observations, we then investigated the effect of SOCS3 overexpression on insulin signaling. As shown in Figure 7A, in response to insulin (10^{-7} M), a significant induction of IRS-1 Tyr^{896} and Akt Ser^{473} phosphorylations were observed in HepG2. Overexpression of SOCS3 (HepG2^{SOCS3} cells) resulted in a reduced activation of both IRS-1 (Figure 7A) and AKT (Figure 7B) in response to insulin. In accordance with previous studies (38), ectopic expression of SOCS-3

appeared to elevate basal autophosphorylation, although this increase was not statistically significant.

Moreover, STAT3 phosphorylation was induced in response to insulin in control cells (HepG2), while SOCS3 overexpression ($HepG2^{SOCS3}$) determined an abrogation of this response (Figure 7C). As previously reported by Costet et al (22), the incubation of HepG2 cells with insulin (10^{-7} M), significantly induced both PCSK9 secretion and mRNA (Figure 8A and 8B), and the presence of SOCS3 further up-regulated the response to insulin at the mRNA levels. However, this effect did not translate to a further induction of PCSK9 secretion in the cultured media, as determined by ELISA assay (Figure 8A). Similarly, we observed an additive effect of insulin and SOCS3 on the FAS and SREBP-1 mRNA levels (Figure 8C and D) with no effect on SREBP-2 and HMG-CoA reductase levels (Figure 8E and F).

DISCUSSION

In the present paper, we have tested the hypothesis that the inhibition of the JAK/STAT pathway by SOCS3 could influence the PCSK9 levels in hepatic cell line. The rationale of performing this study is based on at least four previously reported observations: 1) in clinical settings, a positive relationships of apoB-containing lipoproteins and PCSK9 has been observed (24-27); 2) SOCS3 overexpression, in mice, induces SREBP-1 transcriptional activation and *de novo* lipogenesis (6,7); 3) PCSK9 has been shown to be transcriptionally regulated by SREBP-1 and SREBP-2 (22,23); 4) the adipokine resistin and insulin induce SOCS3 and PCSK9 expression in cultured cell lines and animal models (5,39-41).

The first novel aspect that we observed was the induction of PCSK9 in response to the pro-inflammatory cytokine TNF-α, the same factor that efficiently induces SOCS3 and has been implicated in chronic-inflammation associated with IR (42,43). To study the possible link between SOCS3 and PCSK9, we first suppressed the expression of SOCS3 by siRNA in HepG2. By using this approach, we demonstrated that SOCS3 is required for the TNF-α-driven induction of PCSK9. In addition, the silencing of STAT3 blocked the induction of SOCS3, PCSK9, apoB and SCD-1 in response to TNF-α (Figures 1 and 5). Although the effect of pro-inflammatory cytokines on genes regulating the *de novo* lipogenesis has been previously described (42,44), our data, candidates PCSK9 as a gene involved in lipid metabolism regulated by pro-inflammatory cytokine TNF-α, in a SOCS3 dependent manner. We then established an hepatic cell line stably overexpressing SOCS3, the endogenous inhibitor of STAT proteins, and consistently found to be up-regulated in the liver of genetically- and diet-induced obese animal (6,7).

By WB analysis, we demonstrated that SOCS3 overexpression abrogated STAT3 phosphorylation and thus, the JAK/STAT pathway. By using this cellular model, we observed a significant induction of both PCSK9 mRNA and protein. The involvement of both JAK and STAT proteins was then confirmed by the use of selective pharmacological inhibitors, JAK-I and MD77 (36). The suppression of STAT3 by siRNA induced PCSK9, while the opposite effect was seen after the downregulation of SOCS3. In combination with the induction of PCSK9, we also observed increased SREBP-1 processing and a significant up-regulation of the key genes involved in the *de novo* lipogenesis, such as FAS and the SCD-1, together with the apoB mRNA, apoB secretion and intracellular TG. Interestingly, we noticed that PCSK9 was up-regulated in the liver of ob/ob mice, together with SOCS3, possibly supporting the link between these two genes as observed in cultured system. However, being regulated STAT3 by a large number of cytokines, like IL-6 and TNF-α (45), further *in vivo* studies are needed to elucidated the possible role of STAT3 in SOCS3-driven regulation of PCSK9.The consistent and very significant induction of apoB secretion, confirmed the pivotal role of SOCS3 and the related inflammatory pathway, on hypertriglyceridemia. In addition, our observation suggested a possible involvement of PCSK9 on apoB production by hepatic cells and/or by the liver of animal models previously described (46-48). For instance, the physical interaction between PCSK9 and apoB has been shown to increase apoB production, possibly through the inhibition of intracellular apoB degradation (48). Our evidence further delineate

the potential link between PCSK9 and apoB by demonstrating that the inhibition of the JAK/STAT pathway by SOCS3 is a common determinant of their increased production and secretion. Notably, recent findings suggest that PCSK9 may directly induce apoB mRNA levels in enterocytes (49). It is, therefore, possible to speculate that SOCS3 could activate a positive feedback loop by increasing the expression levels of PCSK9, which, in turn, determines the induction of apoB secretion.

Previous studies have established the SREBP-dependent transcriptional activation of PCSK9. Indeed, similarly to the LDLR and other cholesterol-regulated genes, the proximal region of the PCSK9 promoter contains an SRE-1 motif (22,50). In addition, two independent studies have demonstrated that insulin, by inducing SREBP-1c activity, induces PCSK9 both *in vitro* and *in vivo* (22,41). We confirmed this evidence at both mRNA and protein levels, and the combination of SOCS3 and insulin determined a further induction of *de novo* lipogenesis genes, SREBP-1, and PCSK9, with no additive effect on PCSK9 secretion. These results are in agreement with previous studies showing that the inhibition of STAT proteins by SOCS3 suppresses the transcription of SREBP-1 (7). In our study, the transcriptional activation of SREBP-1 was demonstrated by the induction of key genes involved in the lipid synthesis, such as FAS and SCD-1, while SREBP-2 appears to be unaffected by SOCS3 for at least three reasons. The cholesterol biosynthesis was not altered; an opposite regulation of two genes mainly regulated by SREBP-2 was observed (HMG-CoA reductase and LDLR); and the processing from the precursor to the active form of SREBP-2 was not induced in response to SOCS3 overexpression. The involvement of SREBPs was then demonstrated by the fact that the incubation with 25-OH cholesterol, which completely inhibits their activity, abolished PCSK9 expression. The contribution of SREBP-1, over the SREBP-2, in the regulation of PCSK9 was further corroborated by using fatostatin, a selective SREBP-1 inhibitor (35), which completely suppressed the PCSK9 mRNA levels in HepG2^{SOCS3}. The involvement of HNF-1α, on PCSK9 transcriptional regulation has been previously demonstrated (33,51). In the present study, we cannot exclude the involvement of HNF-1α in SOCS3-mediated PCSK9 induction since both protein and mRNA were increased. Moreover, the luciferase assay with the PCSK9 promoter region having either HNF-1 or SRE site mutated, were drastically suppressed. These data suggest a mutual requirement of both SREBP and HNF-1α on transcriptional regulation of PCSK9 (33).

The effect of SOCS3 on PCSK9 transcription, analyzed in HepG2 and HepG2^{SOCS3} transiently expressing the PCSK9 promoter-driven luciferase reporters PCSK9-D4 (33), found, unexpectedly, that this functional promoter was unresponsive to SOCS3 overexpression (Figure 2L). These results suggest that the SOCS3 response sequences could possibly locate upstream of the promoter region considered. On this regard, it is important to mention that the link between JAK/STAT pathway and PCSK9 has been previously investigated in the same cell line by the use of the cytokine oncostatin M (52). Similar to our study, oncostatin M did not affect the PCSK9 promoter activity (52). Since previous studies have shown that PCSK9 transcription is controlled through cis regulatory elements located in the proximal promoter region of the PCSK9 gene where the Sp1 sites and HNF1 and SRE-1 are located (23,33,51) we utilized also a PCSK9-D4 containing a mutation for the HNF responsive element. Under this condition, we detected a significant increase of the promoter activity in HepG2^{SOCS3} cells. These observation potentially related to the SREBP pathway, activated in response to STAT inhibition, although the overall activity was very low and potentially not responsible for the induction of PCSK9 mRNA levels (7). This effect was also not confirmed with the incubation of the JAK inhibitor, most likely because of the minor inhibition of the pathway in comparison to the complete block after SOCS3 overexpression.

We also exclude a SOCS3 effect on mRNA stability in the induction of PCSK9, since incubation with the transcriptional inhibitor actinomycin D did not affect mRNA stability compared to HepG2. Hence, additional analysis are required to better define the effect of SOCS3 on the transcriptional regulation of PCSK9.Several studies have described the effect of SOCS proteins on insulin signaling (1,43,53).

Although the observations may differ by the cell type and by the time considered, the majority of the studies suggests that SOCS proteins control insulin action by reducing the expression of IRS proteins (1,43,53). Indeed, in our experimental conditions, SOCS3 overexpression reduced both IRS-1 and Akt phosphorylation in response to insulin. Moreover, insulin stimulation of $HepG2^{SOCS3}$ determined a further induction of genes related to *de novo* lipogenesis (FAS and SREBP-1), as well as PCSK9. Although this finding has been obtained in *in vitro*, it is conceivable to hypothesize a functional contribution of PCSK9 on the hypertriglyceridemic condition observed in type 2 diabetes mellitus and obesity. Indeed, PCSK9 directly affects the VLDR expression at the adipose tissue determining the accumulation of visceral adipose tissue in mice (54). For such effect, PCSK9 deficient mice show adipocyte hypertrophy, enhanced *in vivo* fatty acid uptake, and ex vivo triglyceride synthesis (54).

In conclusion, in the present study, we provided evidence for the JAK/STAT dependent expression of PCSK9 in hepatic cell line, suggesting the potential molecular basis of the direct relationship between PCSK9 and TG levels observed in clinical trials (24-27).

Conflict of interest: All the authors declare that they have no conflicts of interest with the contents of this article.

Author contribution: MR and NF conceived and coordinated the study, wrote the paper and designed, performed and analyzed all the experiments. CR performed the experiments shown in Figure 1, 2, 3, 4, 5 and 7. CM performed the experiments shown in Figure 1, 2, 3, and 6. RC performed the experiments shown in Figure 2 and 3. AC and PM critical revised the manuscript. JL critical revised the manuscript and provided reagents for PCSK9 promoter activity. All authors reviewed the results and approved the final version of the manuscript.

REFERENCES

1. Galic, S., Sachithanandan, N., Kay, T. W., and Steinberg, G. R. (2014) Suppressor of cytokine signalling (SOCS) proteins as guardians of inflammatory responses critical for regulating insulin sensitivity. *Biochem J* **461**, 177-188
2. Naka, T., Narazaki, M., Hirata, M., Matsumoto, T., Minamoto, S., Aono, A., Nishimoto, N., Kajita, T., Taga, T., Yoshizaki, K., Akira, S., and Kishimoto, T. (1997) Structure and function of a new STAT-induced STAT inhibitor. *Nature* **387**, 924-929
3. Emanuelli, B., Peraldi, P., Filloux, C., Sawka-Verhelle, D., Hilton, D., and Van Obberghen, E. (2000) SOCS-3 is an insulin-induced negative regulator of insulin signaling. *J Biol Chem* **275**, 15985-15991
4. Bjorbaek, C., El-Haschimi, K., Frantz, J. D., and Flier, J. S. (1999) The role of SOCS-3 in leptin signaling and leptin resistance. *J Biol Chem* **274**, 30059-30065
5. Steppan, C. M., Wang, J., Whiteman, E. L., Birnbaum, M. J., and Lazar, M. A. (2005) Activation of SOCS-3 by resistin. *Molecular and cellular biology* **25**, 1569-1575
6. Ueki, K., Kondo, T., and Kahn, C. R. (2004) Suppressor of cytokine signaling 1 (SOCS-1) and SOCS-3 cause insulin resistance through inhibition of tyrosine phosphorylation of insulin receptor substrate proteins by discrete mechanisms. *Molecular and cellular biology* **24**, 5434-5446
7. Ueki, K., Kondo, T., Tseng, Y. H., and Kahn, C. R. (2004) Central role of suppressors of cytokine signaling proteins in hepatic steatosis, insulin resistance, and the metabolic syndrome in the mouse. *Proc Natl Acad Sci U S A* **101**, 10422-10427
8. Elam, M. B., Yellaturu, C., Howell, G. E., Deng, X., Cowan, G. S., Kumar, P., Park, E. A., Hiler, M. L., Wilcox, H. G., Hughes, T. A., Cook, G. A., and Raghow, R. (2010) Dysregulation of sterol regulatory element binding protein-1c in livers of morbidly obese

women is associated with altered suppressor of cytokine signaling-3 and signal transducer and activator of transcription-1 signaling. *Metabolism: clinical and experimental* **59**, 587-598
9. Seidah, N. G., and Prat, A. (2012) The biology and therapeutic targeting of the proprotein convertases. *Nat Rev Drug Discov* **11**, 367-383
10. Abifadel, M., Varret, M., Rabes, J. P., Allard, D., Ouguerram, K., Devillers, M., Cruaud, C., Benjannet, S., Wickham, L., Erlich, D., Derre, A., Villeger, L., Farnier, M., Beucler, I., Bruckert, E., Chambaz, J., Chanu, B., Lecerf, J. M., Luc, G., Moulin, P., Weissenbach, J., Prat, A., Krempf, M., Junien, C., Seidah, N. G., and Boileau, C. (2003) Mutations in PCSK9 cause autosomal dominant hypercholesterolemia. *Nat Genet* **34**, 154-156
11. Ferri, N., Corsini, A., Macchi, C., Magni, P., and Ruscica, M. (2015) Proprotein convertase subtilisin kexin type 9 and high-density lipoprotein metabolism: experimental animal models and clinical evidence. *Translational research : the journal of laboratory and clinical medicine*
12. Ferri, N., Tibolla, G., Pirillo, A., Cipollone, F., Mezzetti, A., Pacia, S., Corsini, A., and Catapano, A. L. (2012) Proprotein convertase subtilisin kexin type 9 (PCSK9) secreted by cultured smooth muscle cells reduces macrophages LDLR levels. *Atherosclerosis* **220**, 381-386
13. McNutt, M. C., Lagace, T. A., and Horton, J. D. (2007) Catalytic activity is not required for secreted PCSK9 to reduce low density lipoprotein receptors in HepG2 cells. *J Biol Chem* **282**, 20799-20803
14. Maxwell, K. N., Soccio, R. E., Duncan, E. M., Sehayek, E., and Breslow, J. L. (2003) Novel putative SREBP and LXR target genes identified by microarray analysis in liver of cholesterol-fed mice. *J Lipid Res* **44**, 2109-2119
15. Guo, Y. L., Liu, J., Xu, R. X., Zhu, C. G., Wu, N. Q., Jiang, L. X., and Li, J. J. (2013) Short-term impact of low-dose atorvastatin on serum proprotein convertase subtilisin/kexin type 9. *Clinical drug investigation* **33**, 877-883
16. Careskey, H. E., Davis, R. A., Alborn, W. E., Troutt, J. S., Cao, G., and Konrad, R. J. (2008) Atorvastatin increases human serum levels of proprotein convertase subtilisin/kexin type 9. *J Lipid Res* **49**, 394-398
17. Huijgen, R., Boekholdt, S. M., Arsenault, B. J., Bao, W., Davaine, J. M., Tabet, F., Petrides, F., Rye, K. A., DeMicco, D. A., Barter, P. J., Kastelein, J. J., and Lambert, G. (2012) Plasma PCSK9 levels and clinical outcomes in the TNT (Treating to New Targets) trial: a nested case-control study. *J Am Coll Cardiol* **59**, 1778-1784
18. Goldstein, J. L., DeBose-Boyd, R. A., and Brown, M. S. (2006) Protein sensors for membrane sterols. *Cell* **124**, 35-46
19. Horton, J. D., Goldstein, J. L., and Brown, M. S. (2002) SREBPs: activators of the complete program of cholesterol and fatty acid synthesis in the liver. *J Clin Invest* **109**, 1125-1131
20. Horton, J. D., Shah, N. A., Warrington, J. A., Anderson, N. N., Park, S. W., Brown, M. S., and Goldstein, J. L. (2003) Combined analysis of oligonucleotide microarray data from transgenic and knockout mice identifies direct SREBP target genes. *Proc Natl Acad Sci U S A* **100**, 12027-12032
21. Dubuc, G., Tremblay, M., Pare, G., Jacques, H., Hamelin, J., Benjannet, S., Boulet, L., Genest, J., Bernier, L., Seidah, N. G., and Davignon, J. (2010) A new method for measurement of total plasma PCSK9: clinical applications. *J Lipid Res* **51**, 140-149
22. Costet, P., Cariou, B., Lambert, G., Lalanne, F., Lardeux, B., Jarnoux, A. L., Grefhorst, A., Staels, B., and Krempf, M. (2006) Hepatic PCSK9 expression is regulated by nutritional status via insulin and sterol regulatory element-binding protein 1c. *J Biol Chem* **281**, 6211-6218
23. Jeong, H. J., Lee, H. S., Kim, K. S., Kim, Y. K., Yoon, D., and Park, S. W. (2008) Sterol-dependent regulation of proprotein convertase subtilisin/kexin type 9 expression by sterol-regulatory element binding protein-2. *J Lipid Res* **49**, 399-409
24. Cariou, B., Langhi, C., Le Bras, M., Bortolotti, M., Le, K. A., Theytaz, F., Le May, C., Guyomarc'h-Delasalle, B., Zair, Y., Kreis, R., Boesch, C., Krempf, M., Tappy, L., and Costet,

P. (2013) Plasma PCSK9 concentrations during an oral fat load and after short term high-fat, high-fat high-protein and high-fructose diets. *Nutrition & metabolism* **10**, 4
25. Lakoski, S. G., Lagace, T. A., Cohen, J. C., Horton, J. D., and Hobbs, H. H. (2009) Genetic and metabolic determinants of plasma PCSK9 levels. *The Journal of clinical endocrinology and metabolism* **94**, 2537-2543
26. Alborn, W. E., Cao, G., Careskey, H. E., Qian, Y. W., Subramaniam, D. R., Davies, J., Conner, E. M., and Konrad, R. J. (2007) Serum proprotein convertase subtilisin kexin type 9 is correlated directly with serum LDL cholesterol. *Clin Chem* **53**, 1814-1819
27. Baass, A., Dubuc, G., Tremblay, M., Delvin, E. E., O'Loughlin, J., Levy, E., Davignon, J., and Lambert, M. (2009) Plasma PCSK9 is associated with age, sex, and multiple metabolic markers in a population-based sample of children and adolescents. *Clin Chem* **55**, 1637-1645
28. Garton, K. J., Ferri, N., and Raines, E. W. (2002) Efficient expression of exogenous genes in primary vascular cells using IRES-based retroviral vectors. *Biotechniques* **32**, 830, 832, 834 passim
29. Ferri, N., Garton, K. J., and Raines, E. W. (2003) An NF-kappaB-dependent transcriptional program is required for collagen remodeling by human smooth muscle cells. *J Biol Chem* **278**, 19757-19764
30. Greco, C. M., Camera, M., Facchinetti, L., Brambilla, M., Pellegrino, S., Gelmi, M. L., Tremoli, E., Corsini, A., and Ferri, N. (2012) Chemotactic effect of prorenin on human aortic smooth muscle cells: a novel function of the (pro)renin receptor. *Cardiovascular research* **95**, 366-374
31. Ferri, N., Colombo, G., Ferrandi, C., Raines, E. W., Levkau, B., and Corsini, A. (2007) Simvastatin reduces MMP1 expression in human smooth muscle cells cultured on polymerized collagen by inhibiting Rac1 activation. *Arterioscler Thromb Vasc Biol* **27**, 1043-1049
32. Corsini, A., Verri, D., Raiteri, M., Quarato, P., Paoletti, R., and Fumagalli, R. (1995) Effects of 26-aminocholesterol, 27-hydroxycholesterol, and 25-hydroxycholesterol on proliferation and cholesterol homeostasis in arterial myocytes. *Arterioscler Thromb Vasc Biol* **15**, 420-428
33. Li, H., Dong, B., Park, S. W., Lee, H. S., Chen, W., and Liu, J. (2009) Hepatocyte nuclear factor 1alpha plays a critical role in PCSK9 gene transcription and regulation by the natural hypocholesterolemic compound berberine. *J Biol Chem* **284**, 28885-28895
34. Norata, G. D., Banfi, C., Pirillo, A., Tremoli, E., Hamsten, A., Catapano, A. L., and Eriksson, P. (2004) Oxidised-HDL3 induces the expression of PAI-1 in human endothelial cells. Role of p38MAPK activation and mRNA stabilization. *British journal of haematology* **127**, 97-104
35. Kamisuki, S., Mao, Q., Abu-Elheiga, L., Gu, Z., Kugimiya, A., Kwon, Y., Shinohara, T., Kawazoe, Y., Sato, S., Asakura, K., Choo, H. Y., Sakai, J., Wakil, S. J., and Uesugi, M. (2009) A small molecule that blocks fat synthesis by inhibiting the activation of SREBP. *Chemistry & biology* **16**, 882-892
36. Masciocchi, D., Villa, S., Meneghetti, F., Pedretti, A., Barlocco, D., Legnani, L., Toma, L., Kwon, B. M., Nakano, S., Asai, A., and Gelain, A. (2012) Biological and computational evaluation of an oxadiazole derivative (MD77) as a new lead for direct STAT3 inhibitors. *Medchemcomm* **3**, 592-599
37. Giunzioni, L., Tavori, H., Covarrubias, R., Major, A. S., Ding, L., Zhang, Y., DeVay, R. M., Hong, L., Fan, D., Predazzi, I. M., Rashid, S., Linton, M. F., and Fazio, S. (2015) Local Effects of Human PCSK9 on the Atherosclerotic Lesion. *The journal of pathology* **(In press)**
38. Pellegrino, S., Ferri, N., Colombo, N., Cremona, E., Corsini, A., Fanelli, R., Gelmi, M. L., and Cabrele, C. (2009) Synthetic peptides containing a conserved sequence motif of the Id protein family modulate vascular smooth muscle cell phenotype. *Bioorganic & medicinal chemistry letters* **19**, 6298-6302
39. Pirvulescu, M., Manduteanu, I., Gan, A. M., Stan, D., Simion, V., Butoi, E., Calin, M., and Simionescu, M. (2012) A novel pro-inflammatory mechanism of action of resistin in human

endothelial cells: up-regulation of SOCS3 expression through STAT3 activation. *Biochem Biophys Res Commun* **422**, 321-326
40. Melone, M., Wilsie, L., Palyha, O., Strack, A., and Rashid, S. (2012) Discovery of a new role of human resistin in hepatocyte low-density lipoprotein receptor suppression mediated in part by proprotein convertase subtilisin/kexin type 9. *J Am Coll Cardiol* **59**, 1697-1705
41. Chorba, J. S., and Shokat, K. M. (2014) The Proprotein Convertase Subtilisin/Kexin Type 9 (PCSK9) active site and cleavage sequence differentially regulate protein secretion from proteolysis. *J Biol Chem* **289**, 29030-29043
42. Hotamisligil, G. S., Shargill, N. S., and Spiegelman, B. M. (1993) Adipose expression of tumor necrosis factor-alpha: direct role in obesity-linked insulin resistance. *Science* **259**, 87-91
43. Torisu, T., Sato, N., Yoshiga, D., Kobayashi, T., Yoshioka, T., Mori, H., Iida, M., and Yoshimura, A. (2007) The dual function of hepatic SOCS3 in insulin resistance in vivo. *Genes to cells : devoted to molecular & cellular mechanisms* **12**, 143-154
44. Adorni, M. P., Favari, E., Ronda, N., Granata, A., Bellosta, S., Arnaboldi, L., Corsini, A., Gatti, R., and Bernini, F. (2011) Free cholesterol alters macrophage morphology and mobility by an ABCA1 dependent mechanism. *Atherosclerosis* **215**, 70-76
45. Cui, Y., Huang, L., Elefteriou, F., Yang, G., Shelton, J. M., Giles, J. E., Oz, O. K., Pourbahrami, T., Lu, C. Y., Richardson, J. A., Karsenty, G., and Li, C. (2004) Essential role of STAT3 in body weight and glucose homeostasis. *Molecular and cellular biology* **24**, 258-269
46. Benjannet, S., Rhainds, D., Hamelin, J., Nassoury, N., and Seidah, N. G. (2006) The proprotein convertase (PC) PCSK9 is inactivated by furin and/or PC5/6A: functional consequences of natural mutations and post-translational modifications. *J Biol Chem* **281**, 30561-30572
47. Ouguerram, K., Chetiveaux, M., Zair, Y., Costet, P., Abifadel, M., Varret, M., Boileau, C., Magot, T., and Krempf, M. (2004) Apolipoprotein B100 metabolism in autosomal-dominant hypercholesterolemia related to mutations in PCSK9. *Arterioscler Thromb Vasc Biol* **24**, 1448-1453
48. Sun, H., Samarghandi, A., Zhang, N., Yao, Z., Xiong, M., and Teng, B. B. (2012) Proprotein Convertase Subtilisin/Kexin Type 9 Interacts With Apolipoprotein B and Prevents Its Intracellular Degradation, Irrespective of the Low-Density Lipoprotein Receptor. *Arterioscler Thromb Vasc Biol*
49. Rashid, S., Tavori, H., Brown, P. E., Linton, M. F., He, J., Giunzioni, I., and Fazio, S. (2014) Proprotein convertase subtilisin kexin type 9 promotes intestinal overproduction of triglyceride-rich apolipoprotein B lipoproteins through both low-density lipoprotein receptor-dependent and -independent mechanisms. *Circulation* **130**, 431-441
50. Dubuc, G., Chamberland, A., Wassef, H., Davignon, J., Seidah, N. G., Bernier, L., and Prat, A. (2004) Statins upregulate PCSK9, the gene encoding the proprotein convertase neural apoptosis-regulated convertase-1 implicated in familial hypercholesterolemia. *Arterioscler Thromb Vasc Biol* **24**, 1454-1459
51. Shende, V. R., Wu, M., Singh, A. B., Dong, B., Kan, C. F., and Liu, J. (2015) Reduction of circulating PCSK9 and LDL-C levels by liver-specific knockdown of HNF1alpha in normolipidemic mice. *J Lipid Res* **56**, 801-809
52. Cao, A., Wu, M., Li, H., and Liu, J. (2011) Janus kinase activation by cytokine oncostatin M decreases PCSK9 expression in liver cells. *J Lipid Res* **52**, 518-530
53. Emanuelli, B., Peraldi, P., Filloux, C., Chavey, C., Freidinger, K., Hilton, D. J., Hotamisligil, G. S., and Van Obberghen, E. (2001) SOCS-3 inhibits insulin signaling and is up-regulated in response to tumor necrosis factor-alpha in the adipose tissue of obese mice. *J Biol Chem* **276**, 47944-47949

54. Roubtsova, A., Munkonda, M. N., Awan, Z., Marcinkiewicz, J., Chamberland, A., Lazure, C., Cianflone, K., Seidah, N. G., and Prat, A. (2011) Circulating proprotein convertase subtilisin/kexin 9 (PCSK9) regulates VLDLR protein and triglyceride accumulation in visceral adipose tissue. *Arterioscler Thromb Vasc Biol* **31**, 785-791

FOOTNOTES

This wok was supported by Fondazione Cariplo grant Rif. 2012-0549 (AC and NF) and Piano di Sviluppo Università degli Studi di Milano 2014 linea B (NF and MR).

The abbreviation used are: FA, fatty-acid; FAS, fatty acid synthase; HMG-CoA, 3-hydroxy-3-methylglutaryl coenzyme; HNF, hepatocyte nuclear factor; LDL, low-density lipoprotein cholesterol; PCSK9, Proprotein Convertase Subtilisin Kexin Type 9; SREBP, sterol regulatory element binding protein; SOCS3, suppressor of cytokine signaling; STAT, Signal Transducer and Activator of Transcription; SRE, sterol regulatory element; SCD, stearoyl-CoA desaturase; TNF-α, tumor necrosis factor; TG, triglycerides; WB, western blot; qPCR, quantitative-PCR

FIGURE LEGENDS

FIGURE 1. TNF-α induces SOCS3 and PCSK9 in HepG2 cells. A and B) HepG2 cells were seeded in MEM/10% FCS and the day after incubated with MEM supplemented with 10% LPDS for 6h and 24h in the presence or absence of different concentrations of TNF-α (0.1, 1 and 10 ng/ml). At the end of the incubation, the total RNA was extracted and mRNA levels of SOCS3 and PCSK9 were determined by qPCR. Inserts of panels A and B) SOCS3 and PCSK9 protein expression were evaluated by WB analysis from total protein extracts of HepG2 cells incubated for 24h with 10 ng/ml of TNF-α. α-tubulin was used as loading control. C) HepG2 cells were seeded in MEM/10% FCS and the day after transfected with siRNA scramble, STAT3 and SOCS3. After 48h, the medium was replaced with MEM with 10% LPDS. After an additional 24h, the protein expression of STAT3 and SOCS3 and α-tubulin were evaluated by WB analysis. D and E) The cells were incubated under the same experimental conditions described for panels A and B, in the presence or absence of 10 ng/ml TNF-α during the last 24h of incubation in MEM with 10% LPDS. At the end of the incubation, the total RNA was extracted and mRNA levels of SOCS3 and PCSK9 were determined by qPCR. Differences between treatments were assessed by Student's t-test and 1-way ANOVA (when necessary), *$p<0.05$; **$p<0.01$; ***$p<0.001$.

FIGURE 2. SOCS3 overexpression induces PCSK9 in HepG2 cells. A) HepG2 cells were retrovirally transduced with empty retroviral vector or encoding for human SOCS3. After puromycin selection, the expression of SOCS3 mRNA was evaluated by qPCR in HepG2 and HepG2^{SOCS3} cultured in MEM supplemented with 10% LPDS for 24h. B) Under the same experimental conditions, SOCS3 expression was determined by WB analysis from total cell lysates using an anti-SOCS3 antibody. The membrane was stripped and re-probed with anti-α-tubulin antibody as loading control. C) WB analyses with anti-phospho-STAT3 and anti-STAT3 were performed from the same samples described for panel B. D-F) HepG2 and HepG2^{SOCS3} cells were seeded in MEM/10%FCS and the day after incubated with MEM containing 10%LPDS for 24h. D) PCSK9 mRNA was determined by qPCR. Intracellular (E) and secreted (F) PCSK9 levels were evaluated by WB analysis and ELISA assay, respectively. For the determination of PCSK9 levels with WB analysis the cells were incubated for 24h under serum-free condition. G and H) PCSK9 and SOCS3 mRNA expression levels (qPCR) were determined from total hepatic RNA of male ob/ob (n=5) and C57BL/6 control mice (n=5). I) HepG2 cells were seeded in MEM/10% FCS and the day after transfected with siRNA scramble, SOCS3 and STAT3. After 48h, the medium was replaced with MEM with 10% LPDS. After an

additional 24h the total RNA was extracted and mRNA levels of PCSK9 were determined by qPCR. L) HepG2 and HepG2^{SOCS3} cells were transfected with pGL3-PCSK9-D4 or pGL3-PCSK9-SREmut or pGL3-PCSK9-HNFmut. The day after the transfection the medium was replaced with MEM containing 10%LPDS and, after an additional 24h, luciferase activities were determined by Neolite reagent. Luciferase activities were normalized to the β-galactosidase activity of the cotransfected pCMV-β construct. Differences between groups were assessed by Student's t-test, *p<0.05; **p<0.01.

FIGURE 3. SOCS3-dependent upregulation of PCSK9 mRNA is mainly driven by a transcriptional mechanism. A-D) HepG2 and HepG2^{SOCS3} were seeded in MEM/10%FCS and the day after incubated with MEM containing 10%LPDS for 24h in the presence or absence of 25-OH cholesterol (5μM; A) or fatostatin (40μM; B). The levels of PCSK9 mRNA were then determined by qPCR. C) The levels of SREBP-1, SREBP-2 and HNF-1α were determined by WB analysis. Arrows indicate the active and the precursor forms SREBPs. Two different exposure times were utilized for the precursor and the active form of SREBP-2 that have been shown in two different panels. D) HNF-1α mRNA levels were determined by qPCR; E) HepG2 and HepG2^{SOCS3} were incubated at the indicated times with actinomycin D (5μg/ml) and PCSK9 mRNA determined by qPCR. Differences between treatments were assessed by Student's t-test and 1-way ANOVA (when necessary), *p<0.05 and **p<0.01 HepG2 vs HepG2^{SOCS3}; §p<0.01 25-OH cholesterol vs untreated; #p<0.01 fatostatin vs untreated.

FIGURE 4. Pharmacological inhibition of JAK/STAT pathway induces PCSK9 in HepG2 cells. A-D) HepG2 cells were seeded in MEM/10%FCS and the day after incubated with MEM containing 10%LPDS for 24h in the presence or absence of the STAT3 inhibitor MD77 (10^{-7}M) or E-H) JAK inhibitor JAK1 (10^{-5}M). mRNA levels of FAS (A and E), PCSK9 (B and F), HMG-CoA reductase (C and G), and LDLR (D and H) were determined by qPCR. I) HepG2 cells were transfected with pGL3-PCSK9-D4 or pGL3-PCSK9-SREmut or pGL3-PCSK9-HNFmut. The day after the transfection the medium was replaced with MEM containing 10%LPDS with or without JAK1 (10^{-5}M) and, after an additional 24h, luciferase activities were determined by Neolite reagent. Luciferase activities were normalized to the β-galactosidase activity of the cotransfected pRSV-galactosidase construct. Differences between groups were assessed by Student's t-test. *p<0.05.

FIGURE 5. SOCS3 overexpression induces *de novo* lipogenesis in HepG2 cells. A, B and D) HepG2 and HepG2^{SOCS3} cells were seeded in MEM/10%FCS and the day after incubated with MEM supplemented with 10% LPDS for 24h. mRNA levels of FAS, SCD-1, and apoB were evaluated by qPCR analysis from total RNA. C) Under the same experimental conditions, the SCD-1 expression was determined by WB analysis from total protein extracts. E) HepG2 and HepG2^{SOCS3} were cultured in serum free medium for 24h in the presence or absence of 10^{-7}M insulin, conditioned media was than collected and apoB concentrations determined by ELISA assay. F and G) Under the same experimental conditions described for panel A, the intracellular TG and cholesterol levels were determined in HepG2 and HepG2^{SOCS3} by using an enzymatic assay. The values were normalized for total protein content. H-I) HepG2 cells were seeded in MEM/10% FCS and the day after transfected with siRNA scramble and STAT3. After 48h, the medium was replaced with MEM with 10% LPDS in the presence or absence of 10 ng/ml TNF-α. After an additional 24h, the total RNA were extracted and mRNA levels of SCD-1, apoB and FAS were determined by qPCR. Differences between HepG2 and HepG2^{SOCS3} were assessed by Student's t-test and 1-way ANOVA (when necessary), *p<0.05; **p<0.01; ***p<0.001.

FIGURE 6. Cholesterol biosynthesis is not influenced by SOCS3 in HepG2 cells. A and B) HepG2 and HepG2^{SOCS3} cells were seeded in MEM/10%FCS and the day after incubated with MEM containing 10%LPDS for 24h and HMG-CoA reductase and LDLR mRNA determined by qPCR (A and B, respectively). C) Under the same experimental conditions, HMG-CoA reductase expression was assessed by WB analysis from total protein extracts. D) HepG2 and HepG2^{SOCS3} were cultured

in MEM containing 10%LPDS in the presence of [^{14}C]-Acetate. After 48 hours [^{14}C]-Acetate incorporation into cellular cholesterol was evaluated. Each bar represents the mean±SD of triplicate dishes. Differences between HepG2 and HepG2^{SOCS3} were assessed by Student's t-test, *p<0.05.

FIGURE 7. Effect of SOCS3 on insulin-induced IRS-1, Akt and STAT3 phosphorylation. A-C) HepG2 and HepG2^{SOCS3} were seeded in MEM/10%FCS and starved overnight with serum free medium before stimulation with insulin (10^{-7}M) for 5 and 10 min. WB analysis was then performed from total protein extracts by using anti-pIRS-1, anti-pAkt, anti-pSTAT3, anti-STAT3 and anti-α-tubulin antibodies. Densitometric analysis was than evaluated using the ImageLab^{TM} software. Differences between groups were assessed by 1-way ANOVA.

FIGURE 8. Effect of insulin on PCSK9 expression in HepG2^{SOCS3}. A-F) HepG2 and HepG2^{SOCS3} cells were seeded in MEM/10%FCS and the day after incubated in serum free medium for 24h in the presence or absence of insulin (10^{-7}M). A) At the end of the incubation, the PCSK9 levels in the conditioned media were evaluated by ELISA assay, and mRNA levels of PCSK9, FAS, SREBP-1, SREBP-2 and HMG-CoA reductase were determined by qPCR (B-F). Differences between groups were assessed by 1-way ANOVA.

Table 1. Primer sequence utilized for the qPCR analysis.

Human	
Fatty Acid synthase Forward	5'-GCAAATTCGACCTTTCTCAGAAC-3'
Fatty Acid synthase Reverse	5'-GGACCCCGTGGAATGTCA-3'
HMG-CoA reductase Forward	5'-CTTGTGTGTCCTTGGTATTAGAGCTT-3'
HMG-CoA reductase Reverse	5'-GCTGAGCTGCCAAATTGGA-3'
SOCS3 Forward	5'-GACCAGCGCCACTTCTTCAC-3'
SOCS3 Reverse	5'-CTGGATGCGCAGGTTCTTG-3'
SREBP-1 Forward	5'-CGGAACCATCTTGGCAACA-3'
SREBP-1 Reverse	5'-GCCGGTTGATAGGCAGCTT-3'
SREBP-2 Forward	5'- AGCTGGTCTGTGAAG-3'
SREBP-2 Reverse	5'- CGCAATGGGGTCAGC-3'
HNF-1α Forward	5'-TGGCGCAGCAGTTCACCCAT-3'
HNF-1α Reverse	5'- TGAAACGGTTCCTCCGCCCC-3'
LDLR Forward	5'-GTGTCACAGCGGCG-3'
LDLR Reverse	5'-CGCACTCTTTGATG -3'
PCSK9 Forward	5'-CCTGCGCGTGTCAACT-3'
PCSK9 Reverse	5'-GCTGGCTTTTCCGAAACTC-3'
SCD-1 Forward	5'-CTATACCACCACCACCACCA-3'
SCD-1 Reverse	5'-GGGCATCGTCTCCAACTTAT-3'
apoB Forward	5'-GCAGACTGAGGCTACCATGA-3'
apoB Reverse	5'-AGGATTGTTCCGAGGTCAAC-3'
Mouse	
PCSK9 Forward	5'- AACCTGGAGCGAATTATCCCA-3'
PCSK9 Reverse	5'- TTGAAGTCGGTGATGGTGACC-3'

Figure 1

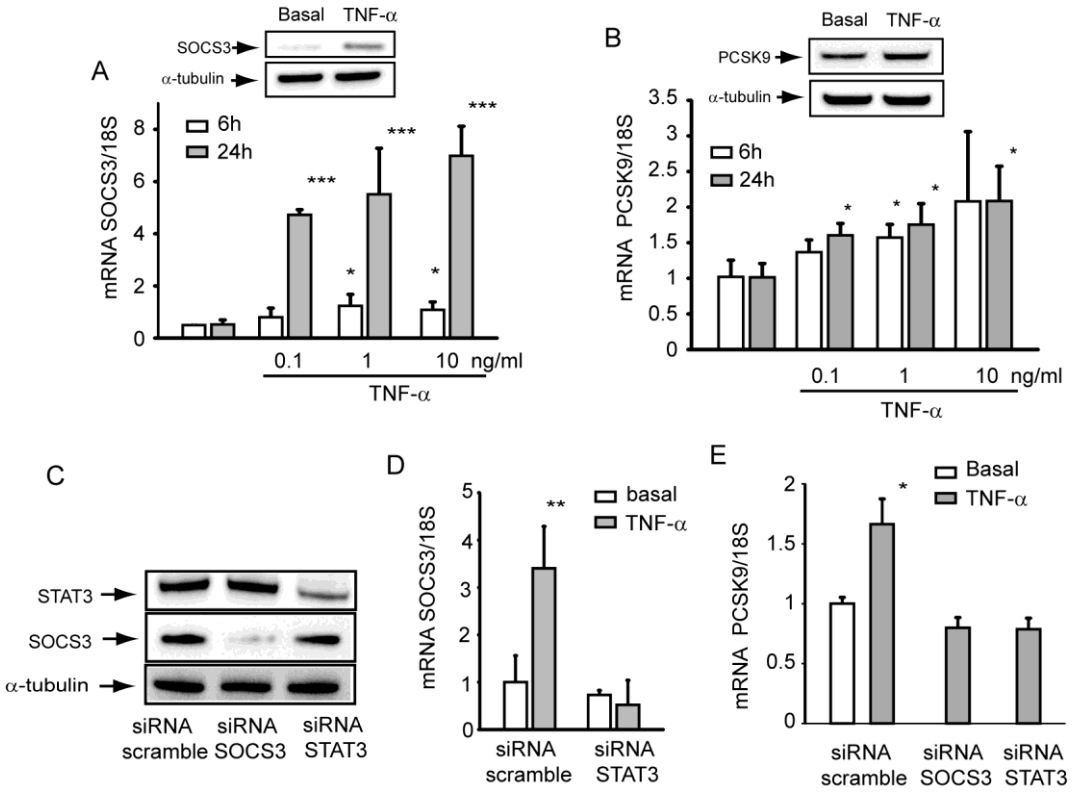

Figure 2

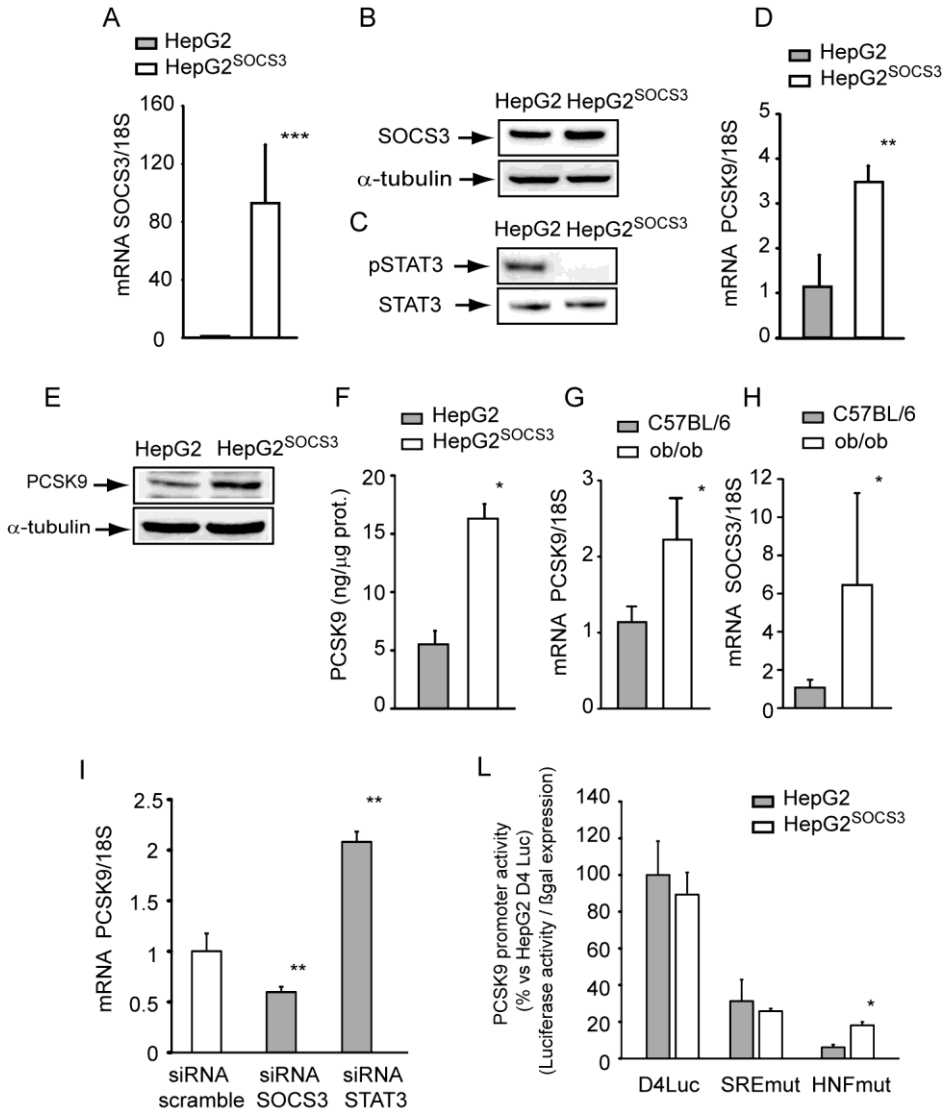

Figure 3

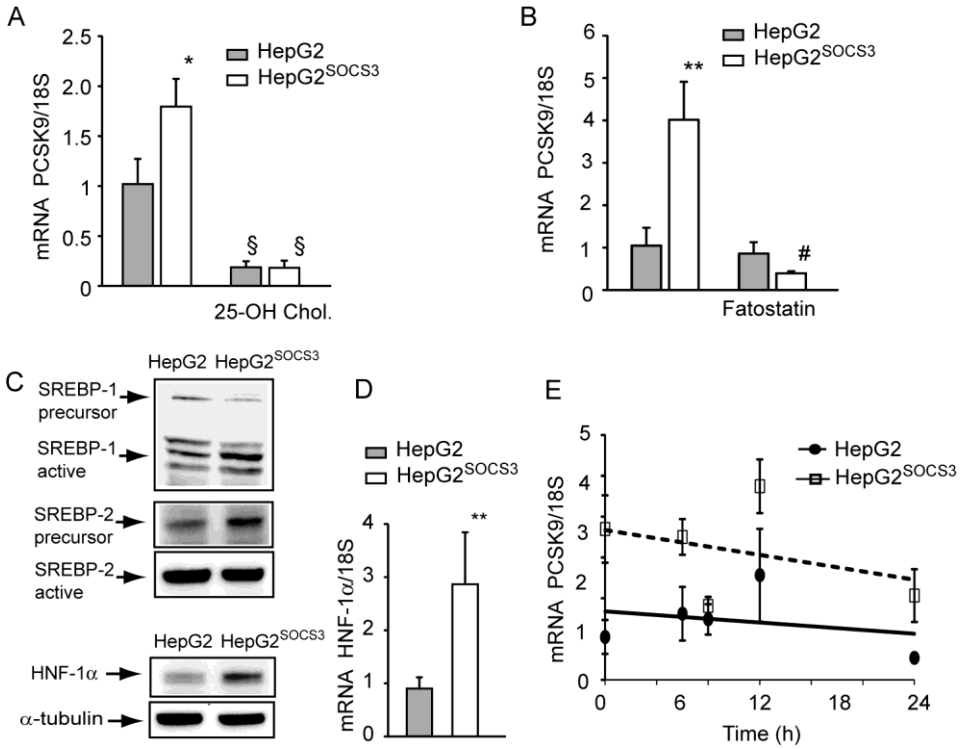

Figure 4

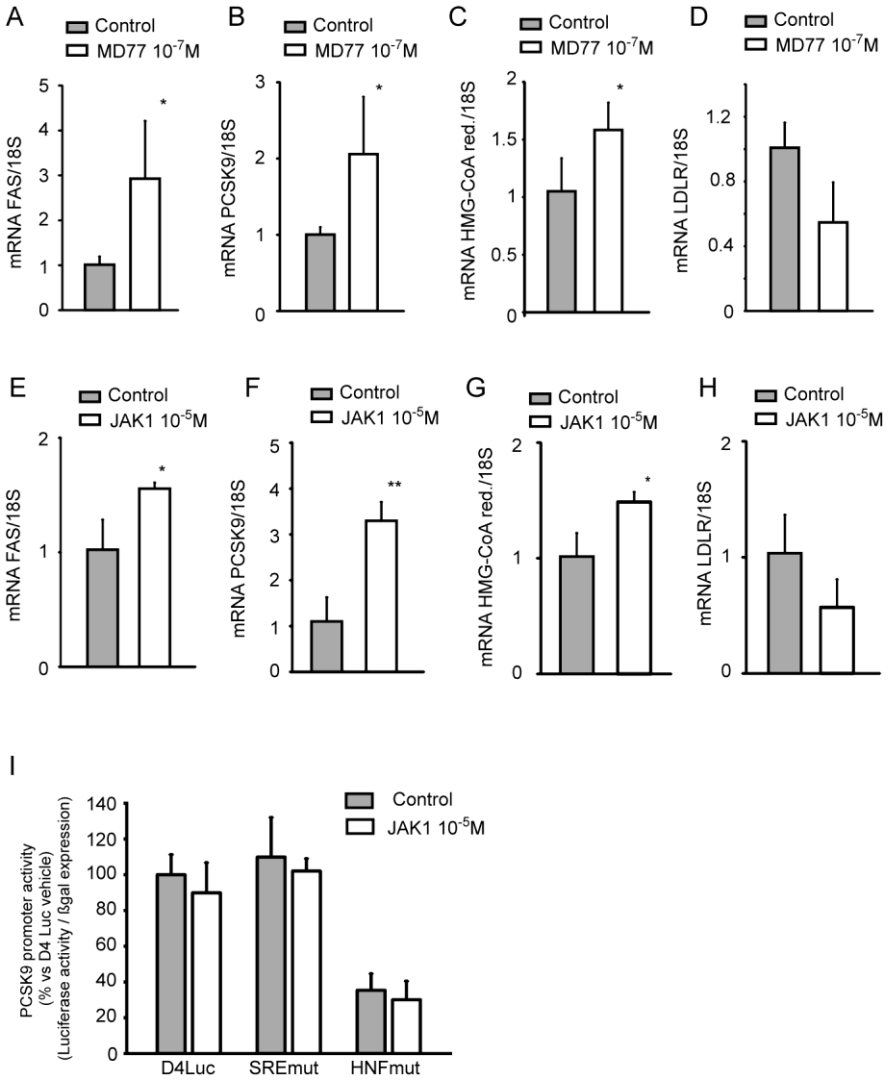

Figure 5

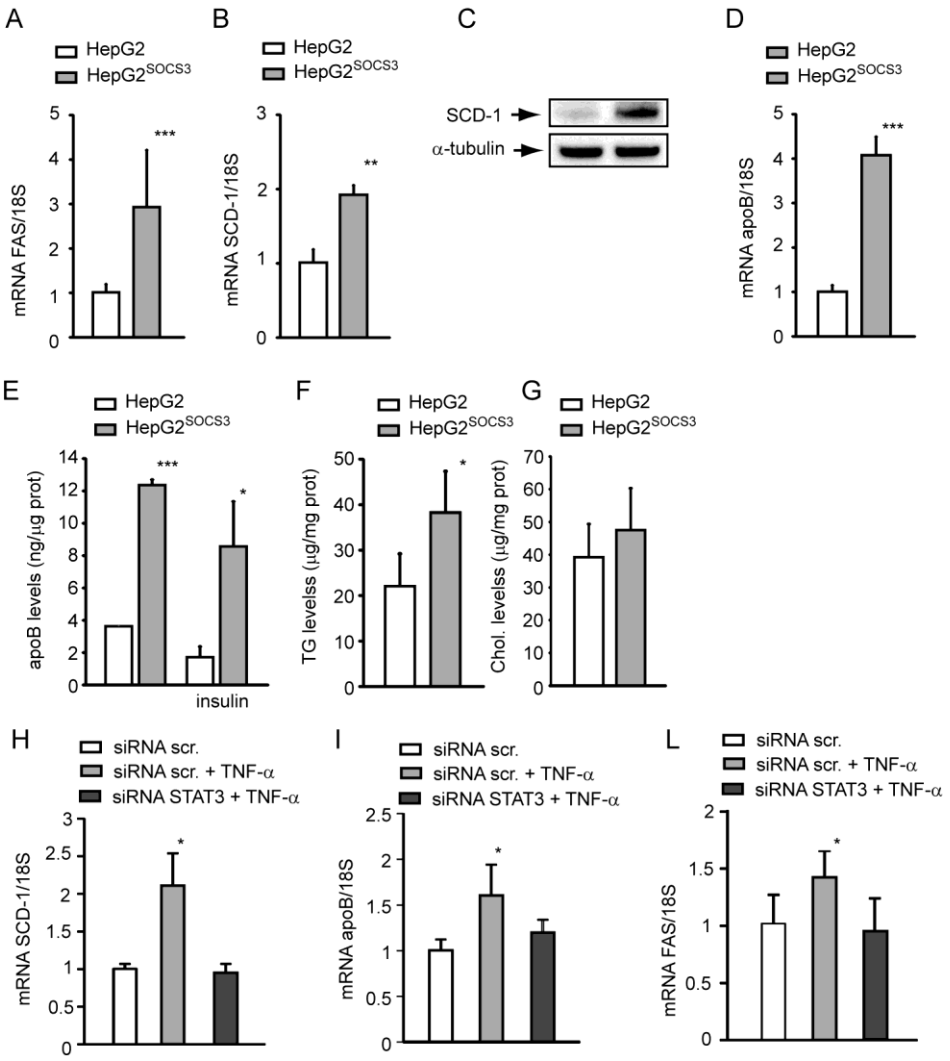

Figure 6

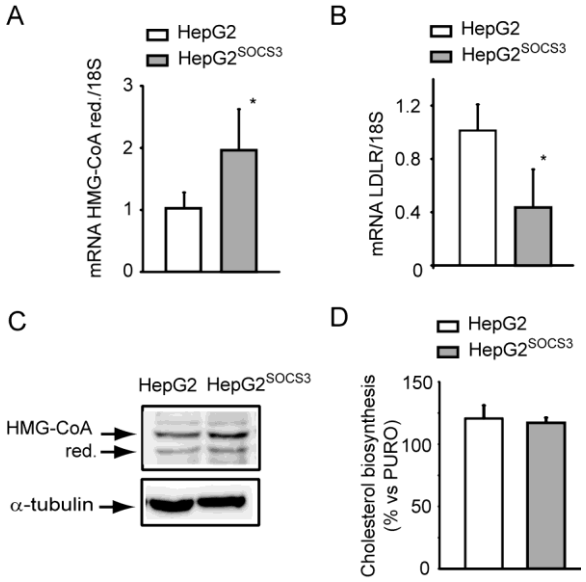

Figure 7

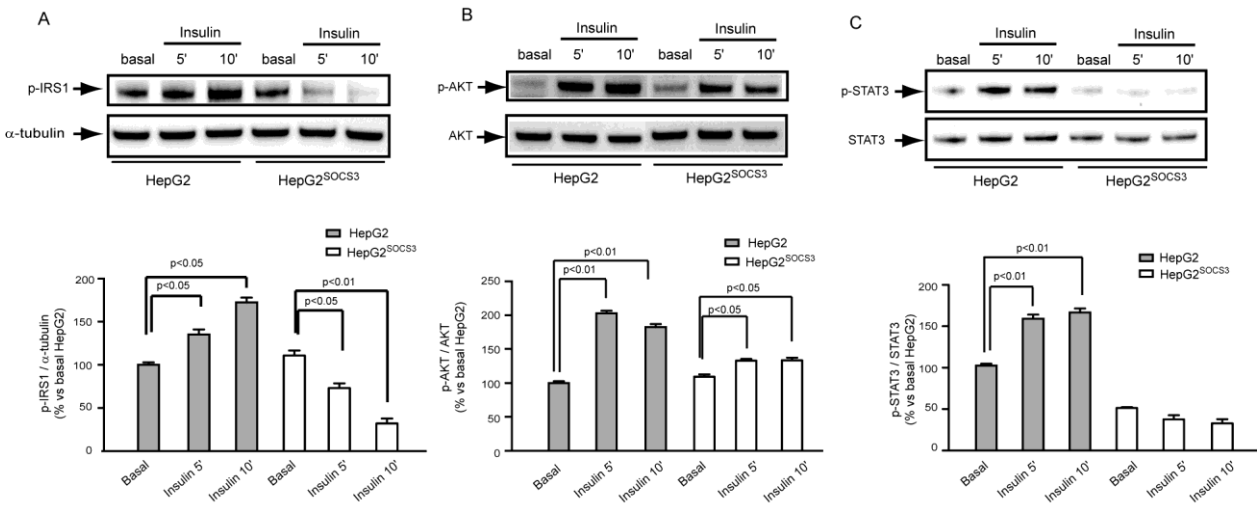

Figure 8

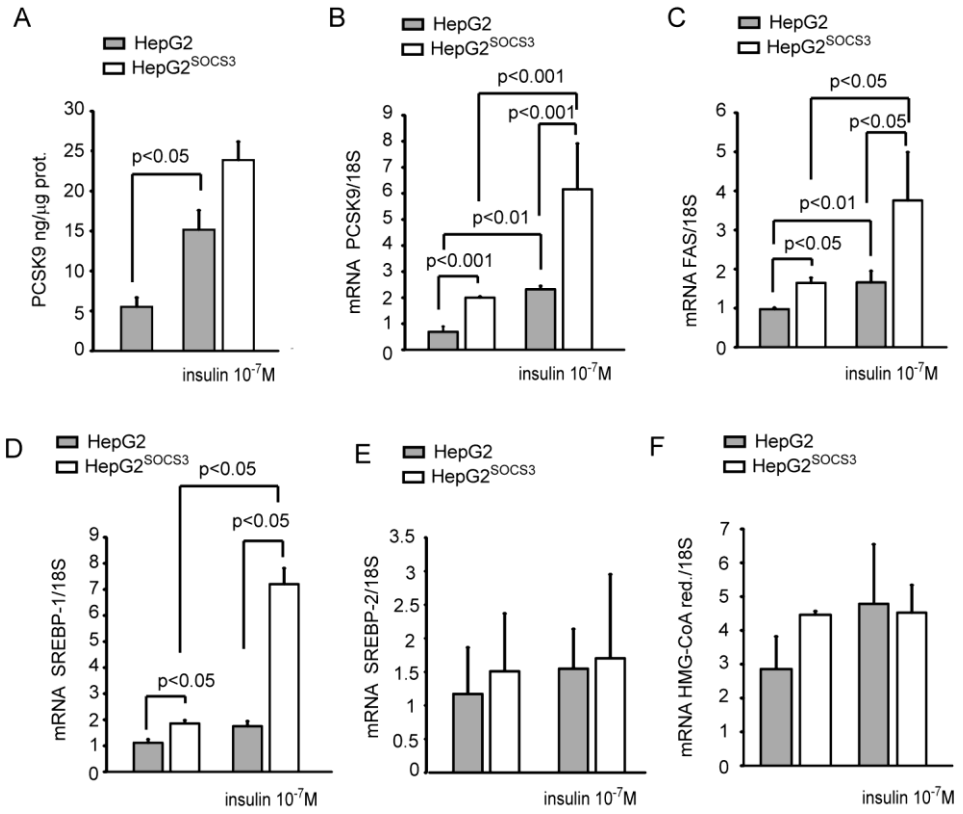

Cell Biology:

Suppressor of Cytokine Signaling-3 (SOCS-3) induces Proprotein Convertase Subtilisin Kexin Type 9 (PCSK9) expression in hepatic HepG2 cell line

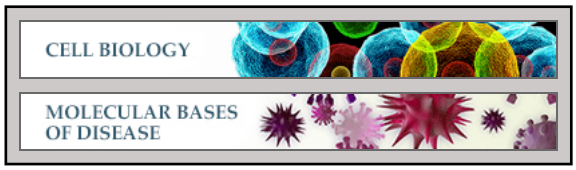

Massimiliano Ruscica, Chiara Ricci, Chiara Macchi, Paolo Magni, Riccardo Cristofani, Jingwen Liu, Alberto Corsini and Nicola Ferri

J. Biol. Chem. published online December 14, 2015